Numerical solution of the time-dependent Schrödinger equation.

Master thesis in Applied and Computational Mathematics

Kjell Nedrelid

Department of Mathematics

University of Bergen

June, 2018

Acknowledgements

I would like to thank my supervisor Professor Magnus Svärd for introducing me to summations by parts and for answering countless questions.

I thank my fellow students for their help and inspiration.

Finally thanks to my family and especially my mom.

Abstract

On the atomic scale the time-dependent Schrödinger equation is used but for systems with three or more particles like the helium atom it is not possible to solve the Schrödinger equation exactly.

The motivation here is to calculate a numerical solution for the helium atom in the ground state. To this end a numerical method must be used and the choice is the summations by part method with simultaneous approximation terms at any boundaries. We analysed and ran numerical verification tests after coding in Matlab on the following PDE's. The transport equation, the heat equation and the Schrödinger equation for particle in a box. The results for the transport equation and the heat equation seems to verify the code but for the particle in a box we seem to very quickly hit the round-off limit and this made the verification difficult for higher order.

We also tested a little on the hydrogen atom before calculating the ground state of helium.

Table of Contents

Introduction and outline

The periodic table of the elements [**1**] includes over 100 known elements and the two lightest elements are hydrogen and helium. While hydrogen is reactive and is found in countless stable molecules helium is only stable as single atoms and the boiling point of helium is 4.2 K. The lack of reactivity of helium motivates taking a closer look on single helium atoms and this is a problem on the atomic scale.

In quantum mechanics the non-relativistic time-dependent Schrödinger equation has a central role and is postulated [**2**] together with a few other postulates. Quantum mechanics explains experimental results for systems on atomic scale, including single sub-atomic particles, atoms and molecules, in physics [**1**] and chemistry. Quantum mechanics seems necessary since Newton's laws of motion does not give accurate results for systems on atomic scale and Newton's laws also fails for relativistic speeds. The Schrödinger equation also fails for relativistic speeds and is replaced with the Dirac equation [**3**]. Since the time-dependent Schrödinger equation is accurate enough in countless non-relativistic experiments including two-particle systems like the hydrogen atom and three-particle systems like the helium atom and we will use the time-dependent Schrödinger equation for the helium atom.

The time-dependent Schrödinger equation is given by

$$i\hbar\frac{\partial\Psi(x,t)}{\partial t} = \hat{H}\Psi(x,t), \qquad x\epsilon\mathbb{R}^N, \qquad t \geq 0, \tag{1.1}$$

where Ψ(x,t) is the wave equation, i is the imaginary unit, $\hbar$ is Planck's reduced constant, $\hat{H}$ is the Hamiltonian operator, x is a vector of space coordinates and N is the number of dimensions. The Hamiltonian operator depends on the specific problem and for a single particle we use

$$\hat{H} = -\frac{\hbar^2}{2m}\nabla^2 + V(x), \tag{1.2}$$

where m is the mass of the particle, ∇^2 is the Laplacian and V(x) is the potential. The Hamiltonian operator is easily extendable to systems of multiple particles including the helium atom. One of the simplest quantum mechanical problems is an electron in one space dimension and the time-dependent Schrödinger equation can for this problem be written as

$$\frac{\partial\Psi'(x',\mathrm{t}')}{\partial t'} = i\left(\frac{1}{2}\frac{\partial^2}{\partial x'^2} - V'(x')\right)\Psi'(x',t'), \qquad a < x' < b, \qquad t' \geq 0, \tag{1.3}$$

where a, b ϵ $\mathbb{R}$ and one or both of a and b can be ± ∞. The ' indicates that all variables are now reduced variables [**4**] also commonly known as dimensionless variables.

This equation is a partial differential equation (PDE) and since this PDE is linear it means that any multiple of a solution is also a solution. Since infinitely many solutions to the PDE is not very useful the PDE must be augmented by some initial and boundary conditions. The augmented problem is well-posed [**5**] if the PDE has an unique solution that depends continuously on any initial and boundary data. We will use the so-called energy method for proving well-posedness of the PDE [**6**].

While we can find analytical solutions for many different potentials for one-particle problems given by equation (1.3), the helium atom is a three-particle system, and none has managed to solve the time-dependent Schrödinger equation for the helium atom or any atoms with more than three particles analytically. We need to use numerical methods instead to solve the time-dependent Schrödinger equation for the helium atom.

In numerical methods neither time nor space are continuous any longer and instead we define a grid where we only know the numerical solution at the grid points and we want the numerical solution to be as close as possible to the exact solution in these grid points. In case we make the spacing between grid-points smaller and smaller we want the numerical solution at the grid points to get closer and closer to the exact solution at the grid points and this is called convergence. We must prove the convergence of the numerical method and due to the Lax-Richtmyer theorem [**7**] we have convergence if we have stability and consistency. We will define both terms in chapter 3.3.

We choose to split the problem in two parts where we use semi-discretisation in space for one of the parts and we afterwards use the classical fourth order explicit Runge-Kutta method for the fully discretised problem. For the semi-discretised system after choosing the grid of space coordinates we need a numerical method that is a good approximation of the PDE at the grid-points and specifically we need a method for calculating the numerical derivative. Of the many possible methods we use the so-called Summation By Parts (SBP) [**8**] method. By using the so-called Simultaneous Approximation Term (SAT) to handle any boundaries at the end of the grid, and even possible between different grids, we can use the energy method for proving the convergence of the SBP-SAT. In SAT instead of setting the numerical solution at any grid points at the boundaries equal to the exact solution at the boundaries, the SAT instead uses a penalty-term where the numerical solution is dragged closer to the exact solution at the grid-point.

Another advantage with using SBP-SAT for the semi-discretised part of the problem is that since we are using a fourth order Runge-Kutta method for the fully discretised problem due to [**9**] if we prove the semi-discretised part converges the fully discretised problem also converges.

Since we want to find the solution for the helium atom and we must use numerical methods for this we need to code this solution on a computer. We code the numerical solution in Matlab and since any kind of coding can include mistakes we need a method to verify the code. We will verify the code by using the transport equation and the heat equation since both PDE has analytical solutions and these are real solutions. We use the time-dependent Schrödinger equation for a particle in a box to verify the code also works for functions with imaginary solutions.

The time-dependent Schrödinger equation for the helium atom includes most of the parts of the hydrogen atom and we use the analytical solution for hydrogen atom in the construction of the function we expect is close to the true solution. Since none have managed finding the true solution of the helium atom we will use the method of manufactured solutions since this makes it possible to do numerical calculations even without the analytical solution.

We have the following outline for the rest of this thesis.

In chapter 2 we analyse well-posedness for the transport equation, the heat equation and the time-dependent Schrödinger equation.

In chapter 3 we start by defining the grid and notation used before we show SBP on matrix form. We analyse the convergence for the semi-discretised numerical solutions for the three PDE in chapter 2.

In chapter 4 we calculate numerical solutions and discuss the results. We start by using the transport equation and the heat equation for verifying the code. We progress to the time-dependent Schrödinger equation for particle in a box and the hydrogen atom in the ground state and finish with the helium atom in the ground state.

In Chapter 5 we give conclusions and discuss possible future work.

Chapter 2: Analysis of well-posedness of PDE's.

We use the following definition for well-posedness of PDE's for a generic PDE written on the form [**10**]

$$u_t(x,t) = P\left(x, \frac{\partial}{\partial x}, t\right)u(x,t) + F(x,t), \qquad a \le x \le b, \qquad t \ge t_0,$$

$$u(x,t) = f(x), \qquad L_a\left(\frac{\partial}{\partial x}, t\right)u(a,t) = g_a(t), \qquad L_b\left(\frac{\partial}{\partial x}, t\right)u(b,t) = g_b(t), \qquad (2.1)$$

where u is the vector function with m components, F(x,t) is the forcing function, $g_a(t)$ and $g_b(t)$ are boundary data, and the terms P, L_a and L_b are differential operators.

Definition 2.1:

Consider the PDE given by equation (2.1) *with F = 0,* g_a *= 0 and* g_b *= 0. We call the problem stable if there is an estimator*

$$\|u(\cdot,t)\| \le Ke^{\alpha(t-t_0)}\|u(\cdot,t_0)\|$$

where K and α are constants that do not depend on f and t_0*. We call it well posed if it has a unique smooth solution and is stable.*

Chapter 2.1: Analysis of the transport equation.

We will here analyse the one-dimensional transport equation on the form given by

$$u_t + cu_x = F(x,t), \qquad a \le x \le b, \qquad t \ge 0, \qquad c > 0, \qquad u \epsilon \mathbb{R},$$
$$u(x,0) = f(x), \qquad (2.2)$$
$$u(a,t) = g_a(t),$$

where a, b and c are real constants, t is time, F(x,t) is the forcing function, f(x) is the initial condition and $g_a(t)$ is boundary data on the left side. All the functions are real functions.

We define the following energy

$$E(t) = \|u(x,t)\|^2,$$

where we will use the L^2 norm, $\|u\| = \int u^* u dx$, and * means adjoint, complex conjugate transposed. By taking the time-derivative of E this gives

$$E'(t) = (\|u(x,t)\|^2)_t = \frac{d}{dt}\int_a^b \big(u(x,t)\big)^* u(x,t)dx.$$

Since u is here real and scalar function we can remove the * in the equation and since a and b are two constants independent of time we can take the time-derivative inside the integral and this gives

$$E'(t) = \int_a^b \frac{\partial}{\partial t}\big(u(x,t)\big)^2 dx = 2\int_a^b u_t(x,t)u(x,t)dx$$

Since PDE in equation (2.2) can be rewritten as $u_t = -cu_x + F$ and F have no effect on the stability we can use F = 0 and this gives

$$E'(t) = -2c \int_a^b u_x(x,t)u(x,t)dx.$$

By using integration by parts we have

$$\int_a^b u_x(x,t)u(x,t)dx = u^2|_a^b - \int_a^b u(x,t)u_x(x,t)dx \Rightarrow 2\int_a^b u(x,t)u_x(x,t)dx = u^2|_a^b,$$

and this gives

$$E'(t) = -cu^2|_a^b = -c\big(u^2(b,t) - u^2(a,t)\big).$$

Since the boundary data at the left boundary will not influence the stability we can set this term to zero and this gives

$$E'(t) = -cu^2(b,t).$$

With $u^2 \geq 0$ and $c < 0$ from equation (2.2) this means $E'(t) \leq 0 \; \forall \; t \geq 0$. Since the derivative of the energy estimate is always negative or zero we know E(t) will be monotonically increasing in this gives

$$E(t) \leq E(0) = \|f(x)\|^2,$$

and we have

$$\|u(x,t)\|^2 \leq \|f(x)\|^2.$$

and since the norm is always zero or positive we have

$$\|u(x,t)\| \leq \|u(x,0)\| = \|f(x)\|.$$

With the choices K = 1, $\alpha = 0$ and $t_0 = 0$ in definition 2.1 the requirements in this definition is fulfilled and this proves the one-dimensional transport equation are well-posed and stable.

We can easily prove uniqueness by assuming we have a different solution v(x,t) of equation(2.2), define w = v-u and we get the following PDE

$$w_t + cw_x = 0, \qquad a \leq x \leq b, \qquad t \geq 0, \qquad c > 0, \qquad u \epsilon \mathbb{R},$$
$$u(x,0) = 0, \qquad u(a,t) = 0,$$

The energy of w follows the steps of the energy of u and with f(x) = 0 we have

$$w(x,t) \geq 0, \qquad w(x,t) \leq 0 \Rightarrow w(x,t) \equiv 0 \Rightarrow u(x,t) \equiv v(x,t),$$

and this proves u and v are the same solution.

Chapter 2.2: Analysis of heat equation and Schrödinger equation.

The PDE we will analyse is given by

$$u_t = c(u_{xx} + V(x)u) + F(x,t), \qquad a < x < b, \qquad t \geq 0, \qquad Re(c) \geq 0,$$
$$u(x,0) = f(x), \qquad a, b, x \epsilon \mathbb{R}, \qquad (2.3)$$
$$u(a,t) = g_a(t), \qquad u(b,t) = g_b(t), \qquad u, F \epsilon \mathbb{C},$$

where V(x) is the real potential in Schrödinger equation, V(x) = 0 in heat equation, g_a, g_b, are boundary data, a and b are two real constants where one or both can be ± ∞, c is a constant with c = i/2 for Schrödinger equation and c > 0 for heat equation.

We define the energy by $E(t) = \|u\|^2$, and take time-derivative and get

$$E'(t) = \frac{d}{dt}\int_a^b u^* u dx.$$

Since a and b are constants independent of time we can take derivative inside the integral and we get

$$E'(t) = \int_a^b u_t^* u + u^* u_t dx.$$

Since the F-term and the boundary data will not influence the stability we set these terms to zero and use PDE in equation (2.3) and this gives

$$E'(t) = \int_a^b \big(c(u_{xx} + Vu)\big)^* u dx + \int_a^b u^* \big(c(u_{xx} + Vu)\big) dx.$$

Remember (AB)*=B*A* and we get

$$E'(t) = c^* \int_a^b u_{xx}^* u + u^* V^* u \, dx + c \int_a^b u^* u_{xx} + u^* V u dx.$$

Since V is real and scalar we can move the terms around and this gives

$$E'(t) = (c^* + c)V \int_a^b u^* u dx + c^* \int_a^b u_{xx}^* u dx + c \int_a^b u^* u_{xx} dx.$$

For the heat equation V = 0 and we can remove the first integral. For the Schrödinger equation c = i/2 and this means c* + c = 0 and we can remove the first integral. For the two remaining integrals we use integration by parts and this gives

$$E'(t) = c^*(u_x^* u)|_a^b - c^* \int_a^b u_x^* u_x dx + c(u^* u_x)|_a^b - c \int_a^b u_x^* u_x dx,$$

and since we said the boundary data does not influence the stability we get

$$E'(t) = -(c^* + c) \int_a^b u_x^* u_x dx.$$

Since c* + c = 2Re(c) this gives

$$E'(t) = -2Re(c) \int_a^b |u_x|^2 dx \leq 0, \qquad Re(c) \geq 0.$$

For the time-dependent Schrödinger equation we get E'(t) ≡ 0, while for the heat equation we get E'(t) ≤ 0. In both cases we know E(t) are either decreasing or constant and this gives

$$E(t) = \|u(x,t)\|^2 \leq E(0) = \|u(x,0)\|^2 = \|f(x)\|^2,$$

and since the norms are always zero or positive this means

$$\|u(x,t)\| \leq \|u(x,0)\|.$$

With the choices K = 1, α = 0 and $t_0 = 0$ in definition 2.1 all the requirements of this definition is fulfilled and we have proven well-posedness of the heat equation and the time-dependent Schrödinger equation.

Chapter 3: Numerical analysis of PDE's.

We need some notations for the grid as a starting-point.

Chapter 3.1: Notation for discretisation.

On the space domain a ≤ x ≤ b we have N grid points and with fixed step-size we have $\mathrm{x_j} = \mathrm{j}\Delta\mathrm{x},\ \mathrm{j} = 0, 1, \dots, \mathrm{N}-1,\ \Delta\mathrm{x} = \frac{\mathrm{b}-\mathrm{a}}{\mathrm{N}-1}$. For t ≥ 0 we use the fixed time-step, Δt, and $t_k = k\Delta t,\ k = 0, 1, 2, \dots$. We can extend to a second space domain by using $y_l = \mathrm{l}\Delta\mathrm{y},\ \mathrm{l} = 0, 1, \dots, \mathrm{N_y}-1,\ \Delta\mathrm{y} = \frac{\mathrm{b_y}-\mathrm{a_y}}{\mathrm{N_y}-1}$.

We want the numerical solution, v, to approximate the exact solution, u, on the grid-points and we use the following notation

$$v_{j,k} \approx u(x_j, t_k), \qquad v_j(t) \approx u(x_j, t),$$

where first form is for full discretisation and second form is for semi-discretised form.

We define the following vectors

$$v(t) = [v_0(t), v_1(t), \dots, v_{N-1}(t)]', \qquad v \epsilon \mathbb{C}^N, \qquad v_j \epsilon \mathbb{C},$$

$$v_k = [v_{0,k}, v_{1,k}, \dots, v_{N-1,k}]', \qquad v_k \epsilon \mathbb{C}^N, \qquad v_{j,k} \epsilon \mathbb{C}.$$

Unless otherwise necessary will use v = v(t) from now on for the semi-discretised form.

We will frequently use the following basis-vectors and basis matrices given by

$$e_j = \begin{bmatrix} 0 \\ 0 \\ \dots \\ 1 \\ 0 \\ \dots \\ 0 \end{bmatrix} \leftarrow position\ j, \qquad E_j = diag(e_j), \qquad j = 0,1, \dots, N-1,$$

where diag(·) means a diagonal matrix with the contents on the diagonal.

Note that $e_j^T v = v_j,\ v^T e_j = v_j,\ E_j v = v_j e_j, v^T E_j = v_j e_j^T$.

Chapter 3.2: The SBP terms.

We need an estimate of the derivative and one method to construct such an estimate is to use central differences given by

$$u_x(x,t) = \frac{u(x+\Delta x, t) - u(x-\Delta x, t)}{2\Delta x},$$

where we can construct these terms by using Taylor series for u(x+Δx,t) and by using two terms in each of the Taylor series we get the error in the estimate is of order $\mathcal{O}((\Delta x)^2)$ when Δx → 0. This is the truncation error, the error from not including an additional term in Taylor serie, and we have a second order estimate of the derivative. We want to use this as a numerical estimate on the grid and this means we want the semi-discretised estimate to fulfil

$$\left(v_j(t)\right)_x \approx u_x(x_j, t),$$

since if true we will have

$$\left(v_j(t)\right)_x \approx \frac{v_{j+1}(t) - v_{j-1}(t)}{2\Delta x},$$

In case the numerical estimate converges to the exact solution when Δx → 0 we have

$$\left(v_j(t)\right)_x = \frac{v_{j+1}(t) - v_{j-1}(t)}{2\Delta x}, \qquad \Delta x \to 0,$$

and this is the SBP term with convergence rate of second order. The convergence rate is a measure of how fast the numerical solution converges to the exact solution at the grid points.

While it is possible to construct SBP-terms with higher convergence rate than second order by using more terms from Taylor series the notation is cumbersome and for this reason we use matrix formulation instead. The definition of SBP on matrix form relies on a matrix called the H-matrix and we will only use H-matrix on diagonal form. The H-matrix is always positive definite and based on [**11**] and [**12**] we have the following definition.

Definition 3.1:

Let $D_1 = H^{-1}Q$ be an SBP operator with internal order 2p and boundary order p. The matrix Q must fulfil $Q + Q^T = E_{N-1} - E_0$. The D_1 operator approximates the first derivative.

Corollary 3.2:

The convergence rate of the solution to equation (2.2) is $min(p+1, 2p)$.

Proof: See [**13**].

The matrices for boundary order 1 is given by

$$H = \Delta x \begin{bmatrix} \frac{1}{2} & & & & \\ & 1 & & & \\ & & \ddots & & \\ & & & 1 & \\ & & & & \frac{1}{2} \end{bmatrix}, \qquad Q = \frac{1}{2} \begin{bmatrix} -1 & 1 & & & & & & & \\ -1 & 0 & 1 & & & & & & \\ & -1 & \ddots & \ddots & & & & & \\ & & \ddots & \ddots & \ddots & & & & \\ & & & \ddots & \ddots & \ddots & & & \\ & & & & \ddots & \ddots & \ddots & & \\ & & & & & \ddots & \ddots & \ddots & \\ & & & & & & -1 & 0 & 1 \\ & & & & & & & -1 & 1 \end{bmatrix},$$

$$D_1 = \frac{1}{\Delta x}\begin{bmatrix} -1 & 1 & 0 & & & & & & \\ -\frac{1}{2} & 0 & \frac{1}{2} & & & & & & \\ & -\frac{1}{2} & 0 & \frac{1}{2} & & & & & \\ & & \ddots & \ddots & \ddots & & & & \\ & & & \ddots & \ddots & \ddots & & & \\ & & & & \ddots & \ddots & \ddots & & \\ & & & & & -\frac{1}{2} & 0 & \frac{1}{2} & \\ & & & & & & -\frac{1}{2} & 0 & \frac{1}{2} \\ & & & & & & 0 & -1 & 1 \end{bmatrix},$$

and for higher orders see [**14**].

Since the Schrödinger equation includes the second derivative we can either use D_1 twice or we need a new operator D_2 as an estimate of the second derivative. We can construct second derivative on component form by adding Taylor series instead of subtracting and this gives

$$\left(v_j(t)\right)_{xx} = \frac{v_{j+1}(t) - 2v_j(t) + v_{j-1}(t)}{(\Delta x)^2}.$$

For the matrix norm based on [**14**] and [**15**] we have the following definition.

Definition 3.3:

If H is diagonal positive definite, A is symmetric positive semi-definite and fulfils $A + A^T \geq 0$, S includes an approximation of the first derivative operator at the boundary then a difference operator

$$D_2 = H^{-1}(-A'' + (E_{N-1} - E_0)S),$$

approximating $\partial^2/\partial x^2$ is a second derivative SBP operator.

Lemma 3.4:

Assume we have diagonal norm H with boundary order p = 1, 2, 3 or 4 and we are using D_2. Then the convergence rate at the boundary of D_2 is p and the global convergence rate is p + 2 except for p = 1 with the global convergence rate is 2. The internal convergence rate of D_2 is 2p.

Proof: See [**16**] and [**14**].

The matrices for boundary order 1 is given by

$$D_2 = \frac{1}{(\Delta x)^2}\begin{bmatrix} 1 & -2 & 1 & & & & & & \\ 1 & -2 & 1 & & & & & & \\ & \ddots & \ddots & \ddots & & & & & \\ & & & & & & & & \\ & & & & & & & & \\ & & & & & & & & \\ & & & & & & 1 & -2 & 1 \\ & & & & & & 1 & -2 & 1 \end{bmatrix},$$

$$S = \frac{1}{\Delta x}\begin{bmatrix} -\frac{3}{2} & 2 & -\frac{1}{2} & & & & & & \\ & 1 & & & & & & & \\ & & \ddots & & & & & & \\ & & & \ddots & & & & & \\ & & & & \ddots & & & & \\ & & & & & \ddots & & & \\ & & & & & & \ddots & & \\ & & & & & & & 1 & \\ & & & & & & \frac{1}{2} & -2 & \frac{3}{3} \end{bmatrix}.$$

While we can use the D_1 twice one disadvantage is the global convergence rate is in this instance p + 1 [**14**] and except for boundary order 1 this gives lower global convergence rate compared to using D_2 instead.

Chapter 3.3: Analysis of convergence.

Based on the Lax-Richtmyer theorem [**7**] we have convergence if we have stability and consistency. We will now define stability and consistency and we start with a general numerical estimate on the grid. For the discrete case let F_j, f_j, g_a and g_b be the grid-functions and approximate the solution of equation (2.1) by

$$\left(v_j\right)_t = Q\left(x_j, D, t\right)v_j + F_j, \qquad j = 0, \dots, N-1, \qquad t \geq t_0$$

$$v_j(t_0) = f_j, \qquad L_a(D,t)v_a(t) = g_a(t), \qquad L_b(D,t)v_b(t) = g_b(t). \tag{3.1}$$

Definition 3.5:

Consider equation (3.1) with F = 0, g_a = 0 and g_b = 0. We call the approximation stable if, for all $\Delta x \leq h_0$, there are constants K and α such that, for all t_0 and all $v(t_0)$,

$$\|v(t)\|_H \leq Ke^{\alpha(t-t_0)}\|v(t_0)\|_H$$

Definition 3.6:

Let u(x,t) be a smooth solution of the PDE given by equation (3.1)*. The approximation given by equation (3.1) is accurate of order p, if the restriction to the grid satisfies the perturbed system*

$$\left(u_j\right)_t = Q\left(x_j, D, t\right)u_j + F_j + (\Delta x)^p \tilde{F}_j, \qquad j = 0,1, \dots$$

$$u_j(t_0) = f_j + (\Delta x)^p \tilde{f}_j$$

$$L_a(D,t) = g_a(t) + (\Delta x)^p \tilde{g}_a(t)$$

$$L_b(D,t) = g_b(t) + (\Delta x)^p \tilde{g}_b(t)$$

where

$$\tilde{F}_j, \tilde{f}_j, \tilde{g}_a, \tilde{g}_b, \frac{d\tilde{g}_a}{dt}, \frac{d\tilde{g}_b}{dt}$$

are bounded independent of Δx. If p ≥ 1 then the approximation given by equation (3.1) is called consistent.

Since the SBP terms based on corollary 3.2 and lemma 3.4 has global convergence rates p > 1 and the SBP-terms is on the form of equation (3.1) definition 3.6 is fulfilled. For this reason we only need to prove stability to prove convergence.

Chapter 3.3.1: Convergence analysis of transport equation.

We need a SBP scheme to solve the transport equation given by equation (2.2) and we use the following scheme where $\mathbb{S}$ is from SAT.

$$v_t = -c(D_1 v + H^{-1}\mathbb{S}) + \tilde{F}, \qquad v(0) = \tilde{f}, \qquad \mathbb{S} = \sigma_0(v_0 - g_0)e_0, \tag{3.2}$$

where $\tilde{F}$ and $\tilde{f}$ are two vectors with the same space-discretisation as v and σ_0 is a constant we must specify based on the stability analysis. Remember v is a vector of semi-discretised form and v_0 is a component of this vector. Since the boundary data and $\tilde{F}$ has no effects on the stability we set these two terms to zero, $v_0 e_0 = E_0 v$, and definition 3.1 the scheme is given by

$$v_t = -cH^{-1}(E_{N-1} + (\sigma_0 - 1)E_0)v. \tag{3.3}$$

We now define the energy estimate by

$$E(t) = \|v\|_H^2,$$

where the H-norm is given by $\|v\|_H = \sqrt{v^* H v}$, and this gives E(t) = v*Hv.

By taking the time-derivative this gives

$$E'(t) = v_t^* H v + v^* H v_t,$$

since H is independent of time. We will not insert the scheme in equation (3.3) and this gives

$$E'(t) = (-cH^{-1}(E_{N-1} + (\sigma_0 - 1)E_0)v)^* H v - cv^* H(H^{-1}(E_{N-1} + (\sigma_0 - 1)E_0)v),$$

Since H and E is real and symmetric and c is a real constant and we assume σ_0 is real we can write this as

$$E'(t) = -c(v^* E_0 H^{-1}(\sigma_0 - 1) + v^* E_{N-1} H^{-1})Hv - cv^* H H^{-1}(E_{N-1} + (\sigma_0 - 1)E_0)v.$$

Since H is positive definite matrix we know H is invertible and we can cancel all the H-terms. This gives

$$E'(t) = -c(v^*(\sigma_0 - 1)E_0 v + v^* E_{N-1} v + v^* E_{N-1} v + v^*(\sigma_0 - 1)E_0 v),$$

and we can immediately reshuffle this into

$$E'(t) = -2c(v^* E_{N-1} v + (\sigma_0 - 1)v^* E_0 v).$$

Since v is real we can use the properties of unit vectors and matrices and this gives

$$E'(t) = -2c(v_{N-1}^2 + (\sigma_0 - 1)v_0^2).$$

With c > 0 and since v2 ≥ 0 to guarantee E'(t) ≤ 0 the term $(\sigma_0 - 1) \geq 0$, and this means must choose

$$\sigma_0 \geq 1.$$

This gives E'(t) ≤ 0 and this means $E(t) \leq E(0) = \|v(0)\|_H^2 = \left\|\tilde{f}\right\|_H^2$. This means definition 3.5 is fulfilled with K = 1, α = 0 and t_0 = 0 and this proves the stability of the semi-discretisation for the transport equation. Since consistency is fulfilled for SBP this proves convergence for the semi-discretisation based on Lax-Richtmyer theorem [**7**].

For the fully discretised problem we use the following assumptions and theorem.

Assumption 3.7:

If λ = iα, $|\alpha| < R_1$, is a solution of $P(\mu) = e^{i\phi}$, $\phi\ real$, then there is no other purely imaginary root μ = iβ, $|\beta| < R_1$, with $P(\mu) = e^{i\phi}$.

Theorem 3.8:

Assume that the Runge-Kutta method is locally stable and that the conditions of assumption 3.7 are satisfied. If the semi discrete approximation is stable in a generalized sense, then the totally discretized approximation is stable in the same sense, if $\|kA'\|_H \leq R < R_1$.

Proof: See [**9**].

For the classical fourth order explicit Runge-Kutta method based on [**17**] R_1 is equal 2.58.

For more about stability in the generalised sense see [**9**].

The matrix A' is a method for writing the Runge-Kutta method but finding the actual matrix is difficult. Still where is a connection to the semi-discretised matrix we used in the schema, this is everything in front of v-vector meaning for the scheme in equation (3.3) we have a matrix, A, given by

$$A = -cH^{-1}(E_{N-1} + (\sigma_0 - 1)E_0), \tag{3.4}$$

and we use this A in the Runge-Kutta method and construct a new matrix A'. The exact form of A' is not important but one important point is if A is positive (semi)-definite then A' is positive (semi)-definite and a matrix that is positive (semi)-definite where λ is eigenvalues of the matrix have Re(λ) ≥ 0. If A not positive (semi)-definite, by removing the negative we will have a positive (semi)-definite A-matrix, unless the matrix is indefinite. Since E'(t) ≤ 0 was fulfilled we know -A must be positive (semi)-definite. The Runge-Kutta method includes Re(λ) ≤ 0 as a requirement in the following definition.

Definition 3.9:

The Runge-Kutta method is called locally stable, if there is an $R_1 > 0$ such that the open half circle $\mathcal{L}(R_1) = \{\lambda\ with\ |\lambda| < R_1, Re(\lambda) < 0\}$ is contained in Ω.

For a more detailed look on the open half circle and Ω, see [**9**].

The important point here is, we know Re(λ) ≤ 0 based on E'(t), since this can be proven by starting with $v_t = Av$ and multiplying from the left with v^*H^{-1} and after many steps this is proven, we do not know the exact form of A' but both Runge-Kutta and theorem 3.8 uses A' and for both A' includes Δt in some way. Since A based on first order derivatives goes like 1 / Δx we can expect Δt must decrease with the same factor if Δx decreases. Also for second order derivative A goes like $1 / \Delta x^2$ decreasing Δx will have much larger effect on Δt.

In all cases, after we have decided on a specific space-discretisation we can always choose a Δt small enough for both Runge-Kutta method and theorem 3.8 being fulfilled if we have already proven the stability.

Finding a small enough Δt is not the problem in analysis, this is a practical problem for calculations and with these arguments we conclude the completely discretised transport equation is proven convergent.

Chapter 3.3.2: Convergence analysis for the heat and Schrödinger equations.

Both PDE's are given by equation (2.3) and we start with the SBP scheme. This is now given by

$$v_t = c(H^{-1}(-A'' + (E_{N-1} - E_0)S) + H^{-1}S^T(\sigma_a E_0 + \sigma_b E_{N-1}) + V)v$$
$$-cH^{-1}S^T(\sigma_a g_a e_0 + \sigma_b g_b e_{N-1}) + F, \tag{3.5}$$

where V is now a diagonal, real matrix. Since F and the boundary terms have no effect on the stability we set these terms to zero and this gives

$$v_t = c(H^{-1}(-A'' + (E_{N-1} - E_0)S) + H^{-1}S^T(\sigma_a E_0 + \sigma_b E_{N-1}) + V)v. \tag{3.6}$$

We now take the adjoint of both sides of this equation and by using c, σ_a, σ_b are constants or on component-form and additionally H is real and symmetric and S is real this gives

$$v_t^* = c^*(-v^*(A'')^*H^{-1} + v^*S^*(E_{N-1}^* - E_0)H^{-1} + v^*(\sigma_a^* E_0^* + \sigma_b^* E_{N-1}^*)SH^{-1} + v^*V^*). \tag{3.7}$$

The energy estimate using H-norm is given by

$$E(t) = \|v\|_H^2.$$

By taking the time derivative this gives

$$E'(t) = \frac{\partial}{\partial t}(v^*Hv) = v_t^*Hv + v^*Hv_t.$$

By using the terms for v_t from equation (3.6) and v_t^* from equation (3.7) this gives

$$E'(t) = -c^*v^*(A'')^*H^{-1}Hv + c^*v^*S^*(E_{N-1}^* - E_0^*)H^{-1}Hv$$
$$+c^*v^*(\sigma_a^* E_0^* + \sigma_b^* E_{N-1}^*)SH^{-1}Hv + c^*v^*V^*Hv - cv^*HH^{-1}A''v$$
$$+cv^*HH^{-1}(E_{N-1} - E_0)Sv + cv^*HH^{-1}S^T(\sigma_a E_0 + \sigma_b E_{N-1})v + cv^*HVv.$$

Since H is invertible this gives

$$E'(t) = -c^*v^*(A'')^*v + c^*v^*S^*(E_{N-1}^* - E_0^*)v$$
$$+c^*v^*(\sigma_a^* E_0^* + \sigma_b^* E_{N-1}^*)Sv + c^*v^*V^*Hv - cv^*A''v$$
$$+cv^*(E_{N-1} - E_0)Sv + cv^*S^T(\sigma_a E_0 + \sigma_b E_{N-1})v + cv^*HVv.$$

Since E_0, E_{N-1} and A'' are real and symmetric we can remove all stars on these terms and since S is real we have $S^T = S^*$ and this gives

$$E'(t) = -c^*v^*A''v + c^*v^*S^*(E_{N-1} - E_0)v$$
$$+c^*v^*(\sigma_a^* E_0 + \sigma_b^* E_{N-1})Sv + c^*v^*V^*Hv - cv^*A''v$$
$$+cv^*(E_{N-1} - E_0)Sv + cv^*S^*(\sigma_a E_0 + \sigma_b E_{N-1})v + cv^*HVv.$$

By some reshuffling of terms this gives

$$E'(t) = -(c^* + c)v^*A''v + v^*S^*((c\sigma_a - c^*)E_0 + (c\sigma_b + c^*)E_{N-1})v$$
$$+v^*((c^*\sigma_a^* - c)E_0 + (c^*\sigma_b^* + c)E_{N-1})Sv + v^*(c^*V^*H + cHV)v. \tag{3.8}$$

Since A'' is positive semi-definite and Re(c) ≥ 0 we know first term is always ≤ 0. The easiest way to be sure E'(t) ≤ 0 is by letting most of the other terms be zero and by requiring the following two terms to be zero we have

$$c\sigma_a - c^* = 0, \qquad c\sigma_b + c^* = 0.$$

We now define $c = c_r + ic_i$ and this gives

$$c_r\sigma_a - c_r + ic_i\sigma_a + ic_i = 0, \qquad c_r\sigma_b + c_r + ic_i\sigma_b - ic_i = 0.$$

This can be split into the following four equations

$$c_r(\sigma_a - 1) = 0, \qquad c_r(\sigma_b + 1) = 0,$$
$$ic_i(\sigma_a + 1) = 0, \qquad ic_i(\sigma_b - 1) = 0.$$

If $c_i \neq 0$ from the last equation we get

$$\sigma_a = -1, \qquad \sigma_b = 1,$$

and we must now have $c_r = 0$. If we instead say $c_r > 0$ this gives

$$\sigma_a = 1, \qquad \sigma_b = -1,$$

and we must have $c_i = 0$. Based on this we know the constant c is either real or pure imaginary. For the heat equation we have pure real c and by putting $\sigma_a = 1,\ \sigma_b = -1$ into equation (3.8) this gives

$$E'(t) = -2Re(c)v^*A''v + v^*(c^*V^*H + cHV)v.$$

For the heat equation V ≡ 0 and c = Re(c) > 0 and this gives

$$E'(t) = -2cv^*A''v \leq 0.$$

With E'(t) ≤ 0 we know E(t) is monotonically increasing or constant and this gives

$$E(t) \leq E(0) = \|v(x,0)\|_H^2 = \|f(x)\|_H^2,$$

and this proves we can choose K, α and t_0 such that definition 3.5 is fulfilled and this proves the semi-discretisation for the heat equation is stable.

For the Schrödinger equation c must be pure imaginary and by putting $\sigma_a = -1,\ \sigma_b = 1$ in equation (3.8) this gives

$$E'(t) = -0v^*A''v + v^*S^*((-ic_i + ic_i)E_0 + (ic_i - ic_i)E_{N-1})v$$
$$+v^*((ic_i - ic_i)E_0 + (-ic_i + ic_i)E_{N-1})Sv + v^*(-ic_iV^*H + ic_iHV)v.$$

This means we have

$$E'(t) = ic_iv^*(HV - V^*H)v.$$

Since V is real and diagonal and since H is real and symmetric we have

$$(HV)^* = V^*H^* = VH.$$

We only use diagonal norm H and with H and V both diagonal we know HV is also diagonal and this gives

$$(HV)^* = HV = VH.$$

With H and V both diagonal this means we have

$$E'(t) = 0,$$

and this means E(t) is constant for the Schrödinger equation. We have

$$E(t) \leq E(0) = \|v(x,0)\|_H^2 = \|f(x)\|_H^2,$$

and we can again choose K and α such that definition 3.5 is fulfilled and we have stability for the semi-discretised Schrödinger equation.

With the same arguments as for the transport equation the semi-discretised problem is convergent and the completely discretised problem also fulfils all requirements. This means we have proven the convergence for the heat equation and the Schrödinger equation.

Chapter 3.4: The Kronecker product.

For the helium atom we need a second dimension and we need a method to handle this.

The Kronecker product is used to multiply two arbitrary sized matrices together [**18**] and we have

$$A \otimes B = \begin{bmatrix} a_{11}B & \cdots & a_{1m}B \\ \vdots & \ddots & \vdots \\ a_{n1}B & \cdots & a_{mn}B \end{bmatrix}, \qquad A \epsilon \mathbb{R}^{m \times n}, \qquad B \epsilon \mathbb{R}^{p \times q},$$

and the dimension of $A \otimes B \epsilon \mathbb{R}^{mp \times nq}$. The Kronecker product has the following feature given by

$$(A \otimes B)(C \otimes D) = AC \otimes BD,$$

as long as the two matrix products AC and BD are defined. Two other features if the Kronecker product are given by

$$(A \otimes B)^T = A^T \otimes B^T,$$

$$(A \otimes B)^{-1} = A^{-1} \otimes B^{-1},$$

where the last hold as long as the two matrices A and B are both invertible.

We use the notation where for space discretisation we use N_x grid points in x-direction and N_y grid points in y-direction. We use the notation for the one-dimensional SBP-terms given by

$$D_{1x}, \qquad D_{2x}, \qquad D_{1y}, \qquad D_{2y},$$

where D_{1x} is first derivative SBP in x-direction, D_{2x} is first derivative SBP in x-direction, D_{1y} is first derivative SBP in y-direction etc. We use similar notation for unit vector, unit matrices and identity matrix and this gives

$$e_{0x}, \qquad E_{0x}, \qquad I_{N_x}, \qquad e_{N_x-1,x}, \qquad E_{N_x-1,x},$$

$$e_{0y}, \qquad E_{0y}, \qquad I_{N_y}, \qquad e_{N_y-1,y}, \qquad E_{N_y-1,y}.$$

We can now construct second order matrices by using

$$D_{1x}^{(2d)} = \left(I_{N_y} \otimes D_{1x}\right),$$

where $D_{1x}^{(2d)}$ is now a two-dimensional SBP-term. The other SBP-terms and SAT can be constructed in a similar fashion.

Chapter 4: Numerical results.

For the SBP-terms based on diagonal norm H the analytical orders we will be using is given in table 4.1 and they are based on corollary 3.2 and lemma 3.4.

Table 4.1: Table of theoretical convergence rates for D_1 and D_2 SBP operators:

Boundary order	Internal order	D_1 global order	D_2 global order
1	2	2	2
2	4	3	4
3	6	4	5
4	8	5	6

Based on the numerical results for two different number of grid-points for the same space-domain we can calculate the numerical convergence rate called the q-factor by using the following equation

$$q = \frac{log\,\frac{\|v^1 - u\|}{\|(v^2 - u)\|}}{\log(\frac{N^1}{N^2})},$$

where 1 is for the smaller number of grid-points and 2 is for the larger number of grid-points. We will use the H-norm and the infinity-norm in the calculations. Remember, the infinity norm for a vector is given by $\|v\|_\infty = \max_{0\le j\le N-1} |v_j|$.

We use the classical fourth order Runge-Kutta method for time-stepping. This method is given by

$$F_1 = \Delta t L(v_k, t), \qquad k = 0,1, \dots,$$

$$F_2 = \Delta t L(v_k + 0.5F_1, t + 0.5\Delta t),$$

$$F_3 = \Delta t L(v_k + 0.5F_2, t + 0.5\Delta t),$$

$$F_4 = \Delta t L(v_k + F_3, t + \Delta t),$$

$$v_{k+1} = v_k + \frac{F_1 + 2F_2 + 2F_3 + F_4}{6},$$

where v_k is a vector and L is a function we need to supply to Runge-Kutta. We construct L from the semi-discretisation and we use the SBP scheme shown previously. We construct L from

$$L = Av_k + c',$$

where A is a matrix and c' is a vector. For the transport equation we have already constructed A in equation (3.4) and this is given by $A = -cH^{-1}(E_{N-1} + (\sigma_0 - 1)E_0)$. The full scheme is given in equation (3.2) and the part not included in A is given by

$$c' = cH^{-1}\sigma_0 g_0 e_0 + \tilde{F},$$

and this is the part of SBP-SAT that is not multiplied with v_k. The L for the transport equation is now given by

$$L = -cH^{-1}(E_{N-1} + (\sigma_0 - 1)E_0)v_k + c\sigma_0 g_0 e_0 H^{-1} + \tilde{F}.$$

From the analysis we found the semi-discretisation was stable for $\sigma_0 \geq 1$ and we use the choice $\sigma_0 = 1$, since in this case the L is simplified to

$$L = -cH^{-1}E_{N-1}v_k + cg_0e_0H^{-1} + \tilde{F}. \qquad (4.1)$$

The stability for the Runge-Kutta method follows from the analysis we did in chapter 3.

Chapter 4.1: Verification of transport equation.

We use the one-dimensional transport equation given in equation (2.2) and since u is the exact solution we use the following

$$u(x,t) = \sin\big(4.1\pi(x-t)\big), \qquad 0 \le x \le 1, \qquad 0 \le t < 100,$$

$$f(x) = u(x,0), \qquad g_0(t) = u(0,t), \qquad F = 0, \qquad c = 1,$$

and for time discretisation we use Δt = 7.8×10^{-5}. We use L given by equation (4.1). The number of grid-points in space coordinate are given in table 4.2.

Table 4.2: Results for one-dimensional transport equation showing difference from exact solution.

	$\|v-u\|_H$ for boundary order				$\|v-u\|_\infty$ for boundary order			
N	1	2	3	4	1	2	3	4
16	1.05E+00	2.06E-01	1.59E-01	1.56E-01	2.30E+00	4.04E-01	4.03E-01	3.26E-01
32	1.80E-01	1.39E-02	1.32E-02	5.34E-03	4.42E-01	2.85E-02	2.84E-02	1.25E-02
64	4.01E-02	1.41E-03	9.74E-04	1.70E-04	9.71E-02	2.69E-03	1.60E-03	4.45E-04
128	9.67E-03	1.63E-04	6.22E-05	4.82E-06	2.33E-02	3.40E-04	8.55E-05	1.07E-05
256	2.39E-03	1.97E-05	3.86E-06	1.43E-07	5.75E-03	4.28E-05	5.29E-06	2.75E-07
512	5.93E-04	2.43E-06	2.40E-07	4.35E-09	1.43E-03	5.37E-06	3.28E-07	8.40E-09
1024	1.48E-04	3.02E-07	1.50E-08	1.34E-10	3.57E-04	6.72E-07	2.04E-08	2.59E-10
2048	3.70E-05	3.77E-08	9.33E-10	4.17E-12	8.92E-05	8.41E-08	1.28E-09	8.13E-12

We see from table 4.2 where is a significant advantage in using the fourth order at the boundary method for space-discretisation compared to the first order at the boundary method.

The calculated q after 100 seconds is shown in table 4.3.

Table 4.3: Numerical convergence rate q for transport equation.

N	q based in H-norm for boundary order				q based on infinity-norm for order			
16	1	2	3	4	1	2	3	4
32	2.550	3.892	3.587	4.872	2.381	3.826	3.826	4.699
64	2.167	3.305	3.759	4.971	2.186	3.404	4.153	4.817
128	2.052	3.111	3.970	5.140	2.060	2.985	4.225	5.378
256	2.019	3.044	4.007	5.080	2.017	2.991	4.015	5.283
512	2.007	3.019	4.008	5.037	2.007	2.995	4.009	5.030
1024	2.003	3.009	4.005	5.017	2.003	2.998	4.005	5.018
2048	2.002	3.004	4.003	5.008	2.002	2.999	4.003	4.995

Note, in the table the calculated q in a given row is based on N in this row and in the row above.

From table 4.3 we detect some differences in the calculated convergence rates q and the theoretical convergence rates for D_1 in table 4.1. With more than 256 gridpoins the calculated convergence rates q and the theoretical convergence rates for D_1 in table 4.1 agrees and this verifies the D_1 is correctly coded.

We also look on stability over time by calculating the norms of the error between exact and numerically calculated result. The error as a function of time is calculated for every 0.1 seconds. Since

all the results except one result follows the same pattern we only include two of error functions. One is the error based on H-norm for order 1 given in figure 4.1 and the other is the error based on infinity-norm for order 4 given in figure 4.2.

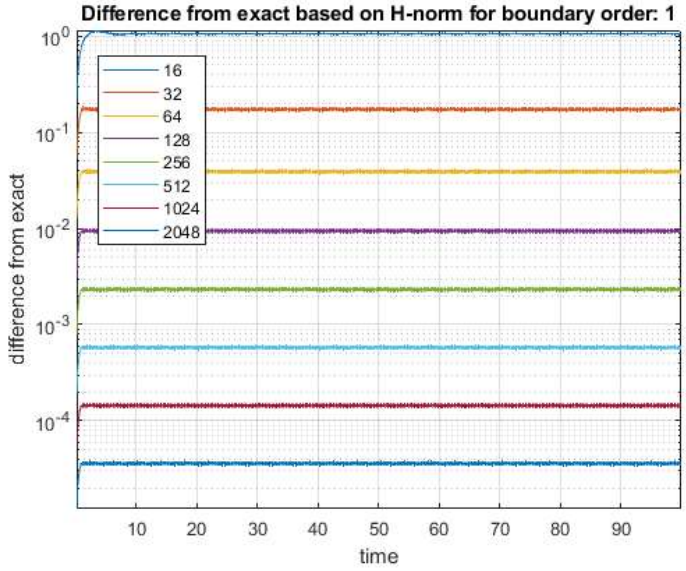

Figure 4. 1: Error as function of time for transport equation.

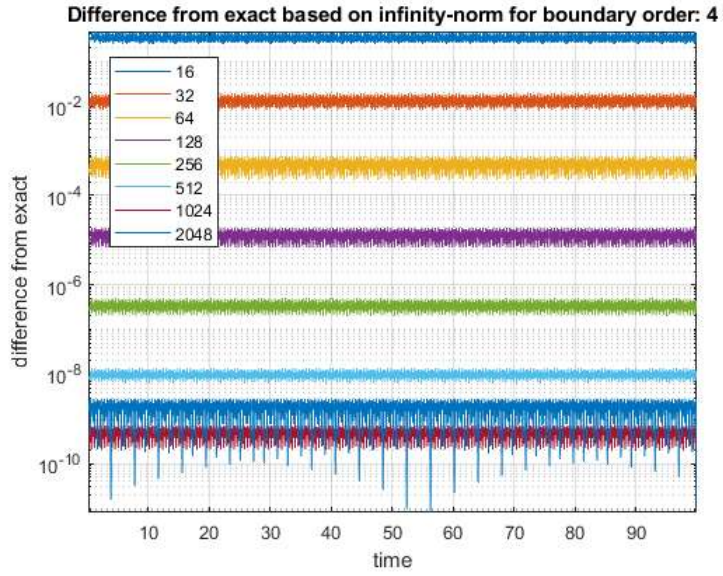

Figure 4. 2: Error as a function of time.

All the results for H-norm follows the pattern in figure 4.1 with good time stability with horizontal graphs but with some small oscillations around these horizontal graphs. All graphs gets more accurate as the number of nodes in space-discretisation increases. The results for infinity-norm follows a similar pattern but with larger oscillations around the horizontal as shown in figure 4.2. One discrepancy is for the fourth order at the boundary the error for N = 2048 is larger than the error for N = 1024 but still looks time stable. Since having a difference around 10^{-10} is a long way from machine epsilon around 10^{-15} we are a long way from this. Still for a single Runge-Kutta time-step by a rough estimate we do around 10^5 calculations and if the errors accumulate we are close to machine epsilon. This indicates where is a maximum number of gridpoints and increasing further will not give any more improvements.

Based on these results we have verified the SBP scheme for the transport equation given in equation (3.2).

We now change the initial condition to $f(x) = 1.5u(x,0)$, and using N = 100 for first order at the boundary after t = 0.5 we have a perturbation of the exact solution and calculated solutions are given in figure 4.4 and we see from this figure running for 0.5 is too short since the influence from initial condition is not fully cancelled. This indicates the method is robust.

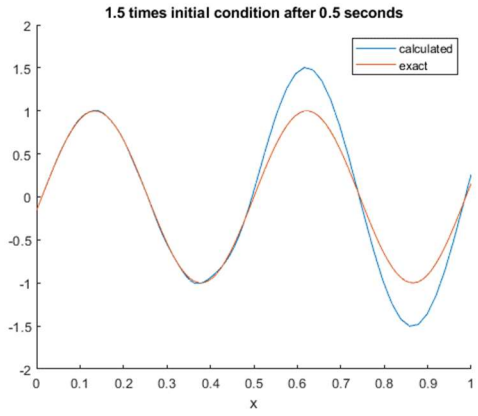

Figure 4. 3: Perturbed problem.

Chapter 4.2: Verification of the heat equation.

We will use the one-dimensional heat equation given by equation (2.3) and we choose the following exact solution given by

$$u(x,t) = 0.25\sin(2\pi x - t) + \sin(t), \qquad 0 \le x \le 1, \qquad 0 \le t < 100$$

$$f(x) = u(x,0), \qquad g_0(t) = u(0,t), \qquad g_1(t) = u(1,t), \qquad c = 1.$$

One problem with this choice of exact solution u is this is not an analytical solution. One method to handle this is to use the method of manufactured solutions [**19**]. We will use the PDE in equation (2.3) for explaining the main steps in the method of manufactured solutions. The first step is to add a new function F to one of the sides in the PDE but since the PDE already have the function F we take step two and move terms until F is alone. This gives

$$F = u_t - cu_{xx}, \tag{4.2}$$

and the next step is to choose a solution u and calculate all the necessary derivatives given in the PDE. This means we have

$$u_t = -0.25\cos(2\pi x - t) + \cos(t),$$

$$u_{xx} = -0.25(2\pi)^2\cos(2\pi x - t),$$

and the last step in the method of manufactured solutions is to put these derivatives into equation (4.2) and this gives

$$F = -0.25\cos(2\pi x - t) + \cos(t) + \pi^2\cos(2\pi x - t),$$

$$F = (\pi^2 - 0.25)\cos(2\pi x - t) + \cos(t). \tag{4.3}$$

We also need to construct the L-function for the Runge-Kutta method. With the SBP scheme given in equation (3.5) we get the following

$$A = c(H^{-1}(-A'' + (E_{N-1} - E_0)S) + H^{-1}S^T(\sigma_a E_0 + \sigma_b E_{N-1}) + V)v_k,$$
$$c' = -cH^{-1}S^T(\sigma_a g_a e_0 + \sigma_b g_b e_{N-1}) + F, \qquad (4.4)$$
$$L = Av_k + c',$$

For the heat equation V = 0, $\sigma_a = 1, \sigma_b = -1$, and we use F from equation (4.3). The complete L for the heat equation is now

$$L = Av_k + c',$$
$$A = c\big(H^{-1}(-A'' + (E_{N-1} - E_0)S) + H^{-1}S^T(E_0 - E_{N-1})\big)v_{k,}$$
$$c' = -cH^{-1}S^T(g_a e_0 - g_b e_{N-1}) + (\pi^2 - 0.25)\cos(2\pi x - t) + \cos(t).$$

We use Δt = 1.4×10^{-5} and the grid size in table 4.4. From the table we detect a significant advantage by going to higher orders. The calculated convergence rates q is shown in table 4.5 and in figure 4.4. From these we see the calculated convergence rates based on H-norm agrees with the theoretical convergence rates in table 4.1. The calculated convergence rates based on infinity-norm are on the other hand too high compared to the analytical convergence rates in table 4.4 for second order at the boundary and for fourth order at the boundary.

Table 4.4: Results for the one-dimensional heat equation showing the error.

N	$\|v-u\|_H$ for boundary order #				$\|v-u\|_\infty$ for boundary order #			
0	1	2	3	4	1	2	3	4
20	1.75E-02	1.22E-02	6.39E-03	1.53E-03	2.60E-02	2.60E-02	5.69E-03	1.80E-03
40	3.05E-03	8.03E-04	1.44E-04	1.58E-05	4.32E-03	1.55E-03	1.97E-04	3.00E-05
60	1.29E-03	1.60E-04	1.68E-05	1.31E-06	1.85E-03	2.68E-04	2.52E-05	2.45E-06
80	7.18E-04	5.06E-05	3.77E-06	2.31E-07	1.01E-03	7.74E-05	5.84E-06	4.08E-07
100	4.59E-04	2.07E-05	1.20E-06	6.01E-08	6.38E-04	2.97E-05	1.88E-06	1.00E-07
120	3.19E-04	9.93E-06	4.73E-07	2.00E-08	4.37E-04	1.37E-05	7.44E-07	3.16E-08
140	2.35E-04	5.34E-06	2.16E-07	7.89E-09	3.18E-04	7.11E-06	3.41E-07	1.19E-08
160	1.80E-04	3.12E-06	1.10E-07	3.53E-09	2.42E-04	4.05E-06	1.73E-07	5.14E-09
180	1.43E-04	1.95E-06	6.06E-08	1.73E-09	1.90E-04	2.47E-06	9.55E-08	2.45E-09
200	1.16E-04	1.27E-06	3.56E-08	9.18E-10	1.53E-04	1.59E-06	5.61E-08	1.27E-09

Table: 4.5: Calculated q for the heat equation.

	q for H-norm and order #				q for infinity-norm and order #			
20	1	2	3	4	1	2	3	4
40	2.523	3.920	5.468	6.597	2.590	4.069	4.850	5.903
60	2.127	3.977	5.305	6.134	2.087	4.326	5.074	6.178
80	2.033	4.005	5.194	6.046	2.095	4.320	5.088	6.230
100	2.004	4.015	5.135	6.034	2.081	4.291	5.083	6.305
120	1.993	4.018	5.101	6.032	2.070	4.262	5.075	6.320
140	1.988	4.018	5.080	6.032	2.067	4.236	5.068	6.316
160	1.987	4.018	5.065	6.031	2.057	4.215	5.062	6.305

180	1.986	4.018	5.054	6.030	2.051	4.197	5.057	6.292
200	1.986	4.017	5.047	6.030	2.050	4.181	5.052	6.278

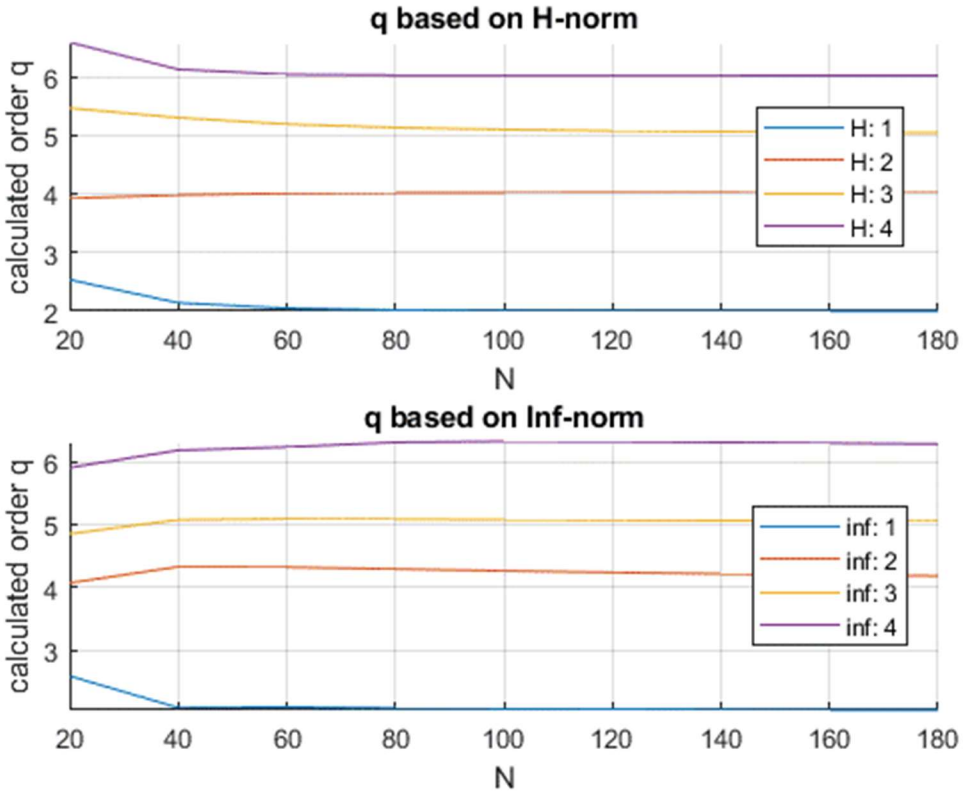

Figure 4. 4: Plotting of q for the heat equation.

We again calculate the difference between numerical and exact solutions for every 0.1 time and the results using H-norm is given in figures 4.5 and figure 4.6 and for infinity-norm in figure 4.7. Since all follows the same pattern with time stability horizontally but some oscillations we will not include the other plots. These oscillations is fairly large and they have they increase for larger number of grid-points. This gives larger gap between two different grids and this is likely the reason for the calculated q being larger than the expected analytically.

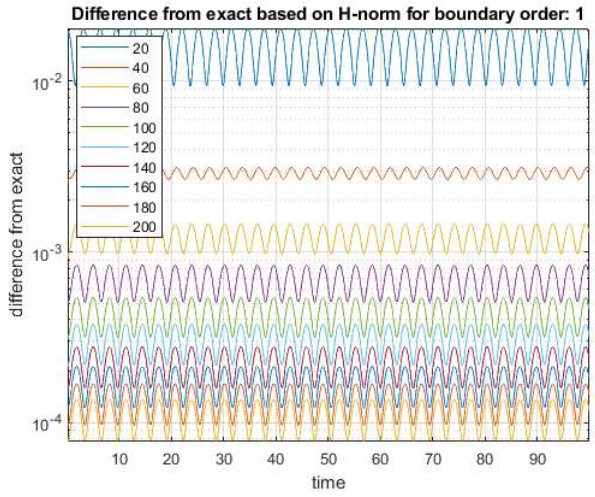

Figure 4. 5: Error over time for the heat equation.

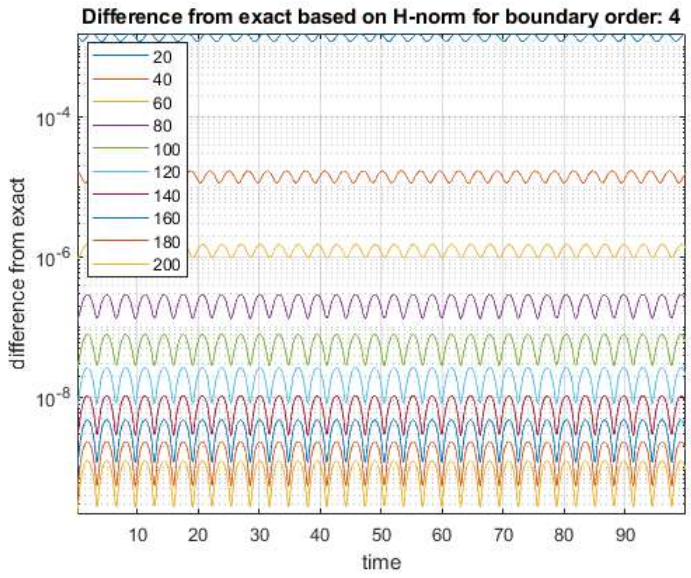

Figure 4. 6: Error over time for the heat equation.

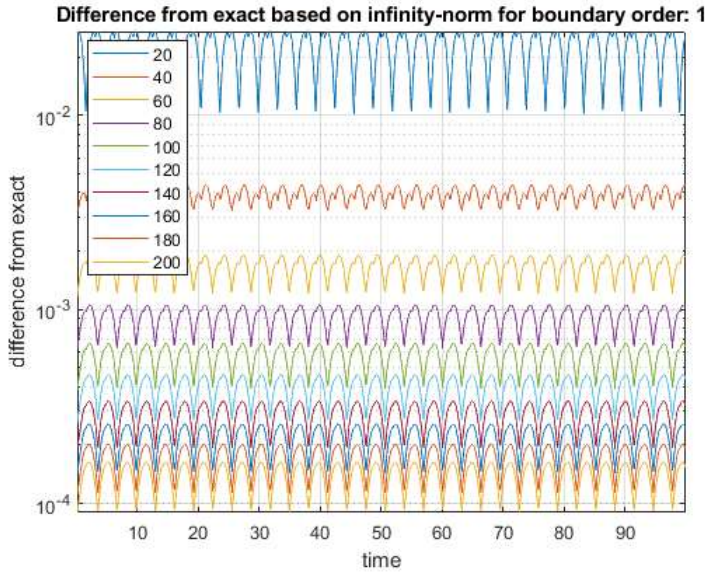

Figure 4. 7: Error over time for heat equation.

Since the q is explained with the larger dips this is a good indication we have verified the one-dimensional heat equation.

Chapter 4.3: Verification of the Schrödinger equation.

The nondimensional Schrödinger equation for an electron in a one-dimensional box is given by

$$u_t = \frac{i}{2}u_{xx}, \qquad 0 \le x \le L, \qquad 0 \le t < t_{max},$$

$$u(0,t) = u(L,t) = 0, \qquad u(x,0) = \sqrt{\frac{2}{L}}\sin\left(\frac{n\pi x}{L}\right), \qquad n = 1,2,\ldots,$$

where t_{max} is the largest time. The analytical solution is given by

$$u(x,t) = \sqrt{\frac{2}{L}}\sin\left(\frac{n\pi x}{L}\right)e^{-iE_n t}, \qquad E_n = \frac{\pi^2 n^2}{2}, \qquad n = 1,2,\ldots$$

We use the following limitations given by

$$L = 1, \qquad n = 1, \qquad 0 \le t < 100, \qquad \Delta t = 4.3 \times 10^{-6},$$

where Δt is used for time discretisation.

We use the same scheme as for the heat equation given in equation (3.5) with one change since F is now zero. The L from equation (4.4) is now given by

$$L = Av_k + c',$$

$$c' = -cH^{-1}S^T(-g_a e_0 + g_b e_{N-1}),$$

$$A = c(H^{-1}(-A'' + (E_{N-1} - E_0)S) + H^{-1}S^T(\sigma_a E_0 + \sigma_b E_{N-1}) + V)v_k.$$

The space discretisation is shown in table 4.6. We see from this table the fourth order at the boundary norms increases when number of grid-points increases past 100 instead of decreasing. This also shows up for the calculated convergence rates in table 4.7 and figure 4.8.

Table 4.6: Error for particle in a box.

N	$\|v-u\|_H$ for boundary order #				$\|v-u\|_\infty$ for boundary order #			
0	1	2	3	4	1	2	3	4
20	1.06E+00	1.40E-03	3.51E-04	1.08E-05	1.49E+00	1.96E-03	4.94E-04	1.56E-05
40	2.66E-01	1.45E-04	2.96E-06	3.36E-08	3.76E-01	2.06E-04	4.20E-06	4.87E-08
60	1.16E-01	3.30E-05	1.76E-07	8.32E-10	1.65E-01	4.68E-05	2.50E-07	1.21E-09
80	6.50E-02	1.11E-05	2.38E-08	1.15E-10	9.19E-02	1.57E-05	3.48E-08	1.96E-10
100	4.14E-02	4.72E-06	5.16E-09	4.31E-11	5.85E-02	6.68E-06	7.61E-09	6.75E-11
120	2.87E-02	2.33E-06	1.39E-09	1.09E-10	4.05E-02	3.29E-06	2.02E-09	1.55E-10
140	2.10E-02	1.28E-06	2.39E-10	8.77E-11	2.97E-02	1.81E-06	8.72E-10	1.25E-10

Table 4.7: Calculated q for particle in a box.

	q H-norm for order #				q for infinity-norm for order #			
20	1	2	3	4	1	2	3	4
40	1.994	3.269	6.892	8.333	1.990	3.252	6.876	8.320
60	2.034	3.653	6.963	9.118	2.033	3.657	6.962	9.125
80	2.027	3.783	6.944	6.885	2.027	3.783	6.849	6.306
100	2.022	3.843	6.860	4.393	2.022	3.842	6.816	4.786
120	2.018	3.877	7.190	-5.066	2.018	3.880	7.275	-4.541
140	2.015	3.901	11.431	1.379	2.015	3.901	5.449	1.399

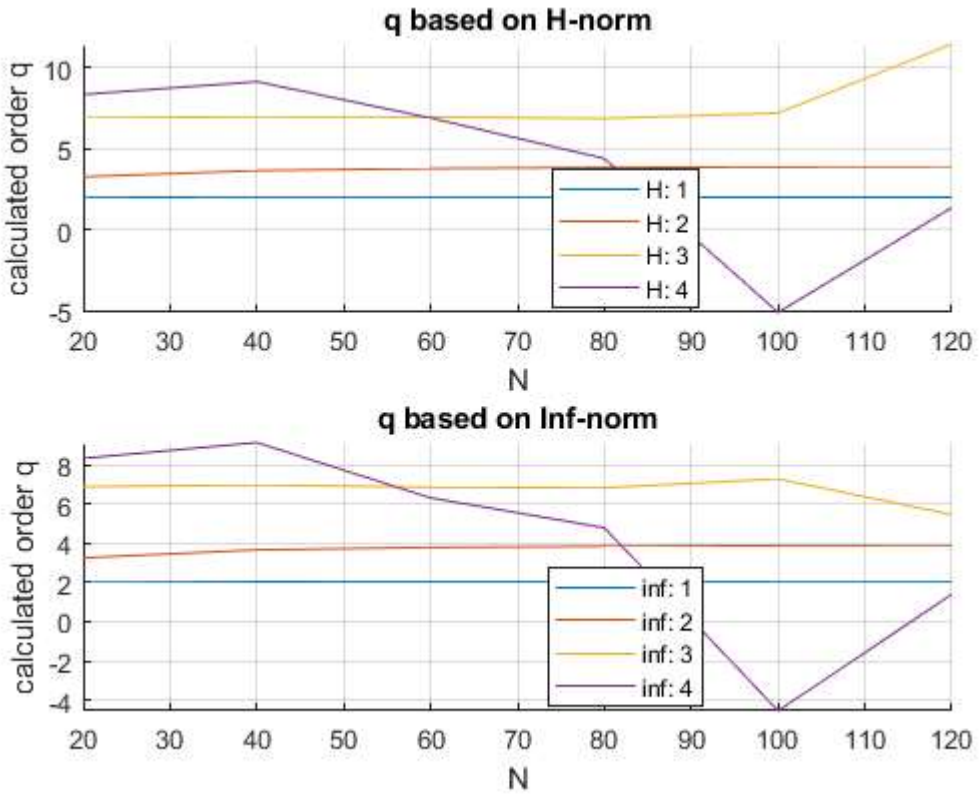

Figure 4. 8: Calculated q for particle in a box.

From table 4.7 we see the two smallest calculated convergence rates are two and close to four and these corresponds to the analytic convergence rates in table 4.1. The next calculated convergence rate is close to seven instead of the analytic convergence rate at six. The highest calculated convergence rate is not stable for either H-norm or infinity-norm.

The difference between numerical results and exact results calculated every 10 timesteps for H-norm is shown in figures 4.9 – 4.12, and for infinity-norm in figures 4.13 – 4.16.

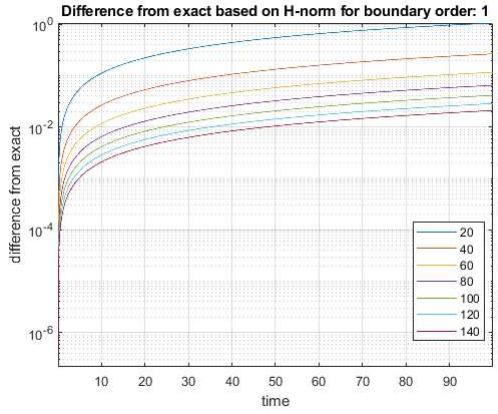

Figure 4. 9

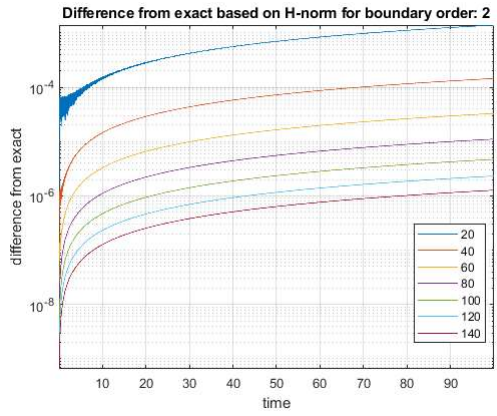

Figure 4. 10

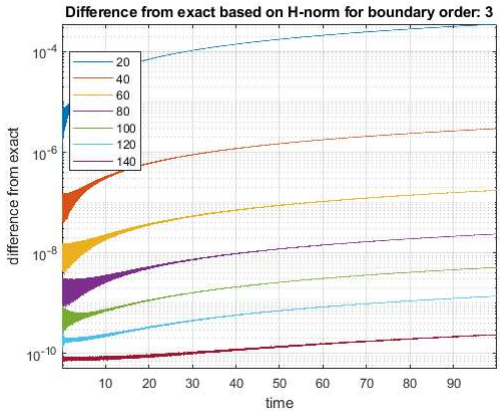

Figure 4. 11

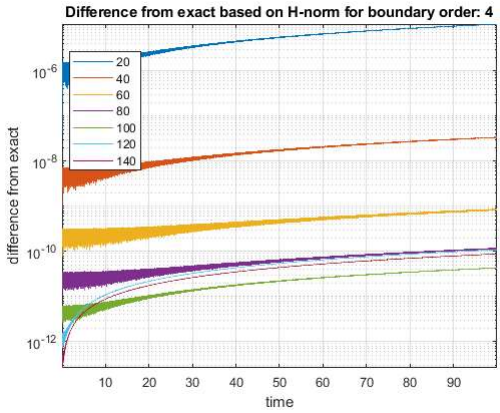

Figure 4. 12

From all these plots one major difference are the error increases with time while for transport equation and heat equation where are only some oscillations with time. The initial increase before the graphs are stable are also much longer and especially third and fourth order at the boundary for infinity-norm is very wide band of errors for fourth order at the boundary the result comes in the wrong order based on increasing number of grid-points.

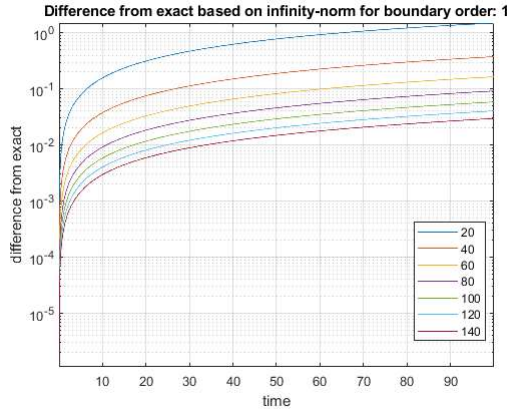

Figure 4. 13

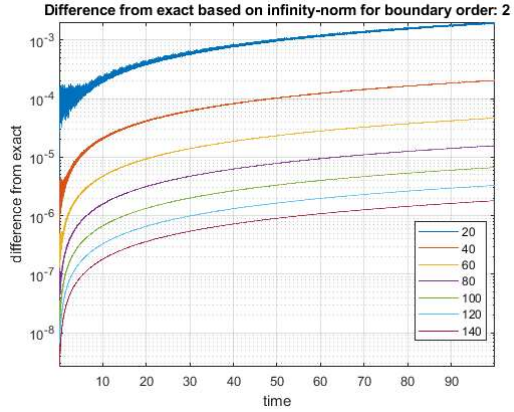

Figure 4. 14

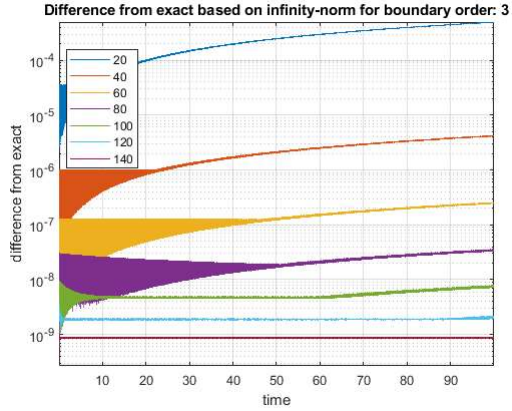

Figure 4. 15

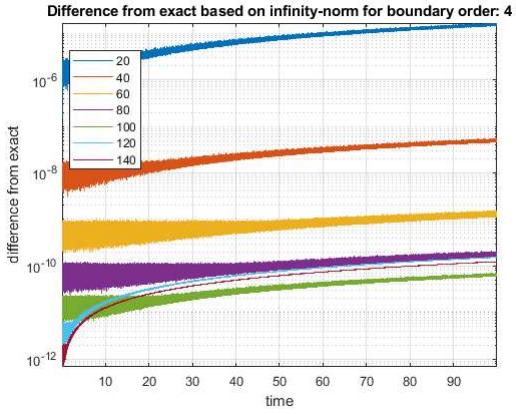

Figure 4. 16

With these results for Schrödinger equation we seem to need large max time, fairly small number of grid-points and the numerically calculated convergence rates are likely off especially for third and fourth order at the boundary. Based on these numerical results we have verified the Schrödinger equation for particle in a box for the two lowest convergence rates at the boundary.

Chapter 4.4: The hydrogen atom.

The hydrogen atom is a two-particle system with a nucleus fixed in origin of a spherical coordinate system and with an electron moving relative to this nucleus. Any atomic ions with a single electron is called a hydrogen-like atom and with the elemental charge on the nucleus given as Z the Schrödinger equation in spherical coordinates are given by

$$i\hbar\frac{\partial\Psi}{\partial t} = -\frac{\hbar^2}{2\mu}\left(\frac{\partial^2}{\partial r^2}+\frac{2}{r}\frac{\partial}{\partial r}+\frac{1}{r^2}\left[\frac{\partial^2}{\partial\theta^2}+\frac{1}{tan\theta}\frac{\partial}{\partial\theta}+\frac{1}{\sin^2\theta}\frac{\partial^2}{\partial\phi^2}\right]\right)\Psi-\frac{Ze^2}{4\pi\epsilon_0}\Psi,$$

where $\Psi = \Psi(r,\theta,\phi,t)$ is the wavefunction in spherical coordinates, μ is the reduced mass of the system, $\frac{1}{4\pi\epsilon_0}$ is a constant in Coulomb potential and e is the elementary charge. The spherical coordinates have radial distance r, $0 \le r < \infty$, polar angle θ, $0 \le \theta \le \pi$, and azimuthal angle φ, $0 \le \varphi < 2\pi$. Everything inside $(\cdot)$ is the Laplacian, ∇^2, written in spherical coordinates. The reduced mass, μ, can be written on the form $\mu = \frac{m_e}{1+\frac{m_e}{m_c}}$, where m_c is the mass of the nucleus. Since the mass of a proton is roughly 1836 times the mass of an electron and all hydrogen atoms includes at least one proton we use the approximation $\mu \approx m_e$. Since all other atoms than hydrogen have an even heavier nucleus this approximation works for all atoms. The wavefunction in hydrogen-like atoms is specified with the tree quantum numbers n, l and ml and we choose l = 0 since we can write the normalised radial Schrödinger equation given by

$$\frac{\partial u}{\partial t} = \frac{i}{2}\left(\frac{\partial^2 u}{\partial r^2}+\frac{2Z}{r}u\right), \qquad u = r\Psi_{\mathrm{n00}}, \qquad 0 \le r < \infty,$$

where Ψ_{n00} means we have the wavefunction with l = 0 and ml = 0. The energy for hydrogen-like atoms only depends on the quantum number n and is given by

$$E_n = -\frac{1}{2}\frac{Z}{n^2}, \qquad n = 1,2,\ldots.$$

With n = 1 and Z = 1 the exact solution of the Schrödinger equation for the hydrogen atom is given by

$$\Psi_{100}(r,t) = \frac{1}{\sqrt{\pi}}e^{-r}e^{-iE_1 t}, \qquad E_1 = -\frac{1}{2}.$$

When we discretise the space-coordinate we also remove the singularity for r = 0 in equation above by using

$$\frac{1}{r} = \left(\frac{1}{r} - \frac{1}{\Delta r}\right), \qquad r \geq \Delta r,$$

$$\frac{1}{r} = 0, \qquad r < \Delta r,$$

where Δr is the size between grid-points in space discretisation.

We use the following when we numerically solve the Schrödinger equation for the hydrogen atom

$$u = r\Psi_{100}, \qquad 0 \leq r \leq 6, \qquad 0 \leq t \leq 12.566,$$

$$u(0,t) = u(6,t) = 0, \qquad u(r,0) = r\Psi_{100}(r,0).$$

Since we use a small domain in space-coordinate while the wavefunction is normalised to infinity we must add a forcing function F(r,t) and we find it by the methods of manufactured solutions. The Schrödinger equation is given by

$$\frac{\partial u}{\partial t} = \frac{i}{2}\left(\frac{\partial^2 u}{\partial r^2} + \frac{2Z}{r}u\right) + F.$$

We use the same scheme as before for the Schrödinger equation given in equation (3.5).

We need the F and this is given by

$$v_t = -iE_1 r\frac{1}{\sqrt{\pi}}e^{-r}e^{-iE_1 t},$$

$$v_{xx} = -\frac{1}{\sqrt{\pi}}e^{-r}e^{-iE_1 t},$$

$$F = -iE_1 r\frac{1}{\sqrt{\pi}}e^{-r}e^{-iE_1 t} + \frac{i}{2}\frac{1}{\sqrt{\pi}}e^{-r}e^{-iE_1 t} - iVv, \qquad V = \frac{1}{r} - \frac{1}{\Delta x},$$

where V is the adjustment for removing the singularity.

We use Δt = 2.1×10^{-5} and number of grid-points are given in table 4.8. Since we do not have an analytical solution any longer we do not have any meaningful convergence rates.

Table 4.8: Error for the hydrogen atom.

N	H-1	H-2	H-3	H-4	inf-1	inf-2	inf-3	inf-4
16	0.03234	0.02522	0.03101	0.02858	0.02626	0.01752	0.02709	0.02373
32	0.05539	0.05453	0.05472	0.05454	0.05099	0.04956	0.04951	0.05052
64	0.01146	0.01156	0.01156	0.01147	0.01296	0.01240	0.01193	0.01041
128	0.01459	0.01430	0.01431	0.01429	0.01533	0.01405	0.01397	0.01456
256	0.00428	0.00447	0.00437	0.00435	0.00694	0.01199	0.01149	0.00975

In figure 4.17 we have the radial solution for 256 grid-points and order 1 at the boundary and we see the abrupt cut-off for the numerical result at the right boundary. We divide the numerical solution with r and the same for exact solution and plot this in figure 4.18. The results for the hydrogen atom is as good as can be expected with the early cut-off with radius 6.

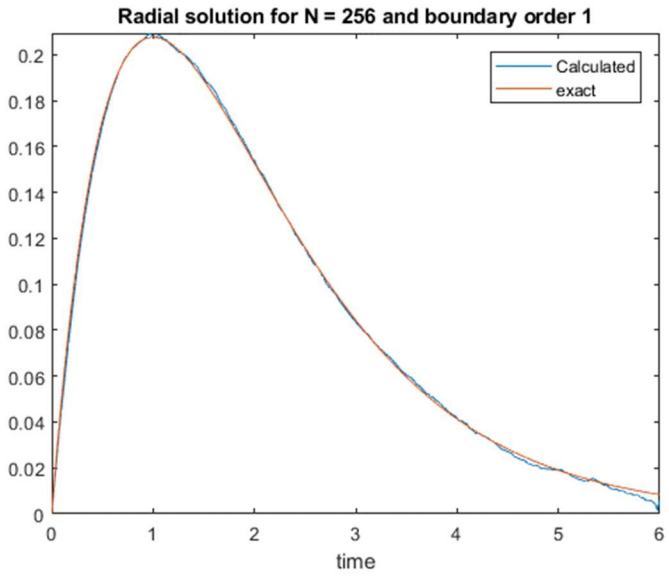

Figure 4. 17: Radial solution for the hydrogen atom.

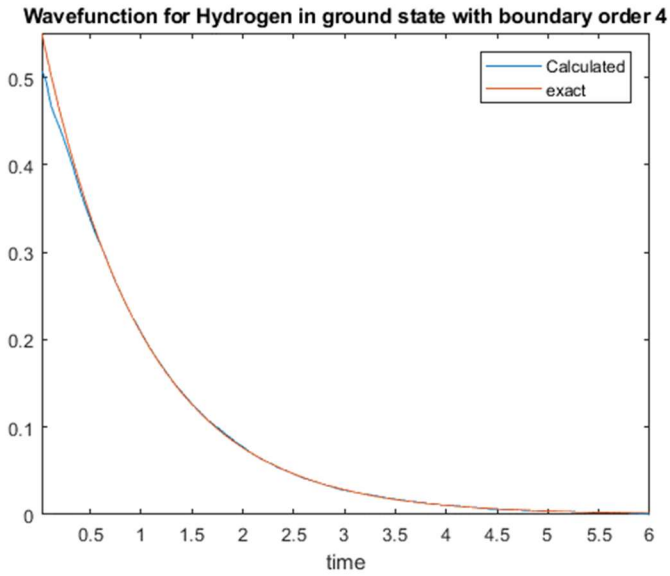

Figure 4. 18: Wavefunction for hydrogen.

Chapter 4.5: The helium atom.

The Helium atom have a heavy nucleus surrounded by two electrons and any other type of atoms ionised to having two electrons is called helium-like atoms. By placing the nucleus in origin and by assuming we can label one of the electrons with 1 and the other electron with 2 we can easily write the Hamiltonian operator given by

$$\widehat{H} = -\frac{\hbar^2}{2\mu}\nabla_1^2 - \frac{Ze^2}{4\pi\epsilon_0 r_1} - \frac{\hbar^2}{2\mu}\nabla_2^2 - \frac{Ze^2}{4\pi\epsilon_0 r_2} + \frac{e^2}{4\pi\epsilon_0 r_{12}}, \qquad r_1, r_2 \epsilon \mathbb{R}^3, \qquad r_{12} = |r_1 - r_2|,$$

where r_1 and r_2 is the radial distances from nucleus to electrons labelled 1 and 2 and r_{12} is the distance between the two electrons. We use the approximation $\mu \approx m_e$ for each of the electrons. The last term, $\frac{e^2}{4\pi\epsilon_0 r_{12}}$, is the Coulomb repulsion between the two electrons. If we neglect this

repulsion term we can separate the variables and solve each electron as a hydrogen-like atom. Since the Coulomb repulsion term is not negligible we must include this term and we have an analytically unsolvable three-particle problem. We must use a numerical solution instead and where are no exact solution to compare with. We will use the method of manufactured solution after we choose our solution.

We are only interested in the ground state and this simplifies the problem in a similar way as for the hydrogen atom. By averaging the spherical component [**20**] and by using the radial function $u = r_1 r_2 \Psi$, we get the nondimensionalised Schrödinger equation for helium-like atoms is given by

$$\frac{\partial u}{\partial t} = i\left(\frac{1}{2}\left(\frac{\partial^2}{\partial r_1^2} + \frac{\partial^2}{\partial r_2^2}\right) + Z\left(\frac{1}{r_1} + \frac{1}{r_2}\right) - \frac{1}{r_{avg}}\right)u + F, \qquad r_{avg} = \max(r_1, r_2),$$

and we use the limits and boundary data given by

$$0 \leq r_1, r_2 \leq 10, \qquad 0 \leq t \leq 4.413,$$

$$u(0, r_2, t) = u(r_1, 0, t) = u(10, r_2, t) = u(r_1, 10, t) = 0.$$

We assume a similar form of the solution as for hydrogen-like atoms and this gives

$$u = \frac{Z^{\frac{3}{2}}}{\sqrt{\pi}} r_1 r_2 e^{-Z(r_1 + r_2)} e^{-iZ^2 t},$$

and we use this u for the initial condition at t = 0.

While the nuclear charge in the helium atom is 2, part of the time one electron will shield for the other electron and we use Z = 27/16 for the helium atom. We use Δt = 6.3×10-5 for the time-discretisation. We use the number of grid points given in table 4.9.

Table 4.9: Error for the helium atom.

N_x	N_y	H-1	H-2	H-3	H-4	inf-1	inf-2	inf-3	inf-4
16	24	3.05E-01	3.58E-02	1.93E-02	7.80E-03	2.92E-01	3.07E-02	2.23E-02	1.50E-02
32	48	1.54E-02	1.61E-02	2.55E-03	2.38E-03	1.44E-02	9.85E-03	1.59E-03	1.51E-03
64	96	3.61E-03	4.20E-03	1.41E-04	4.11E-04	1.77E-03	1.77E-03	7.09E-05	2.68E-04
128	192	1.86E-03	5.53E-04	1.18E-06	2.00E-06	8.41E-04	3.44E-04	2.12E-06	9.55E-07

With no exact solution any plotting of convergence rates are meaningless.

The radial solution of the Schrödinger equation for the helium atom in the ground state for 32 × 48 grid points is given in figure 4.19 and the numerical solutions for the orders 1 – 4 are shown in figures 4.20 – 4.28.

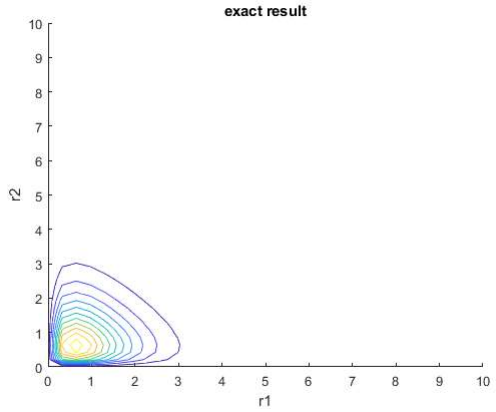

Figure 4. 19: Our guess for exact solution

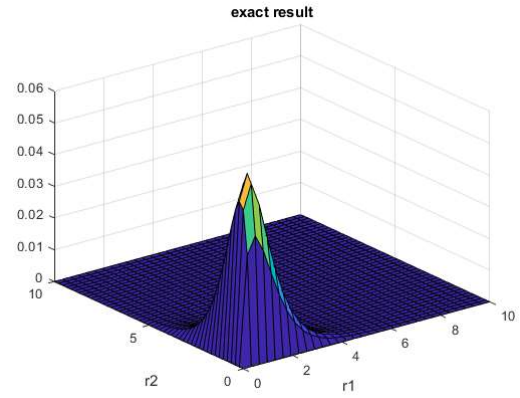

Figure 4. 20: Our guess for exact solution.

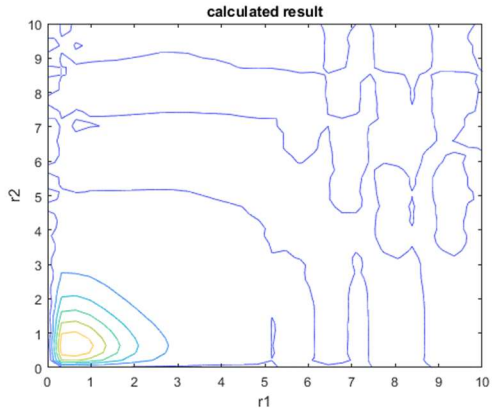

Figure 4. 21: calculated order 1

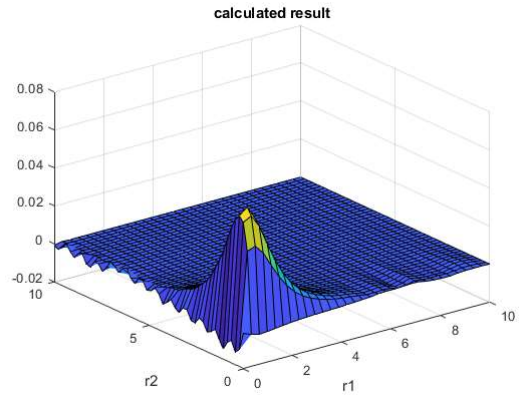

Figure 4. 22: Calculated order 1.

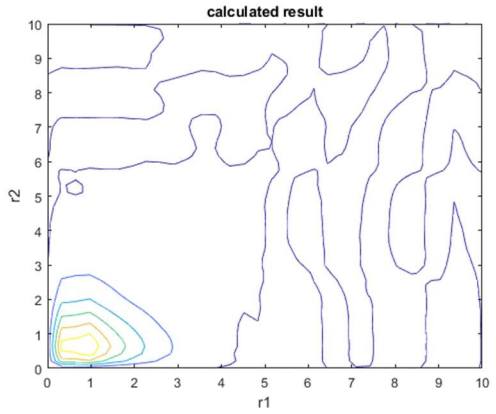

Figure 4. 23: Calculated order 2.

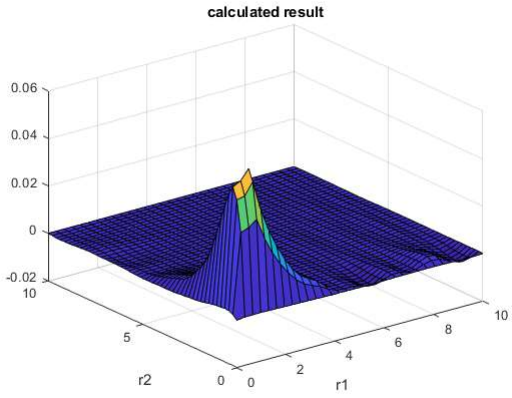

Figure 4. 24: Calculated order 2.

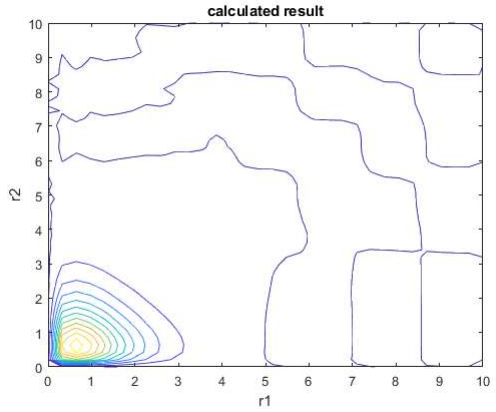

Figure 4. 25: Calculated order 3.

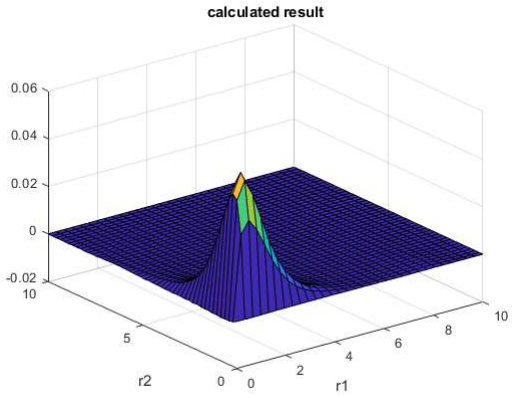

Figure 4. 26: Calculated order 3.

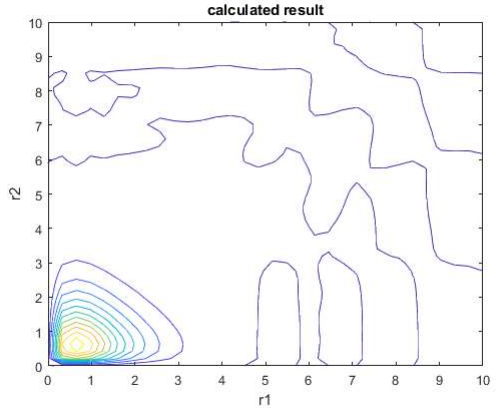

Figure 4. 27: Calculated order 4.

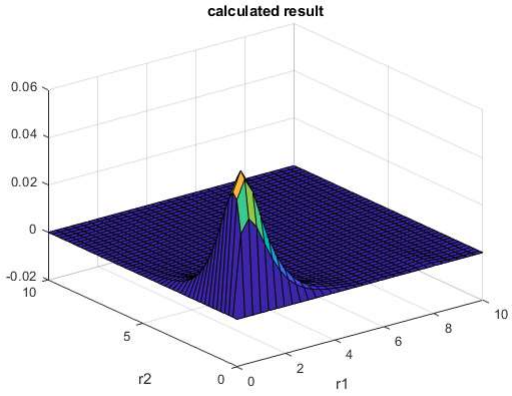

Figure 4. 28: Calculated order 4.

From these figures we see the two lowest orders are markedly different from the exact solution while the two highest orders seem to include all the major features of the exact solution. All numerical solutions include some contours outside the region with contours for the exact solution. This is likely due to the abrupt cutoff we used.

Increasing to 128 × 192 gives similar results and only show the exact in figure 4.29 and the calculated for order 1 in figure 4.30.

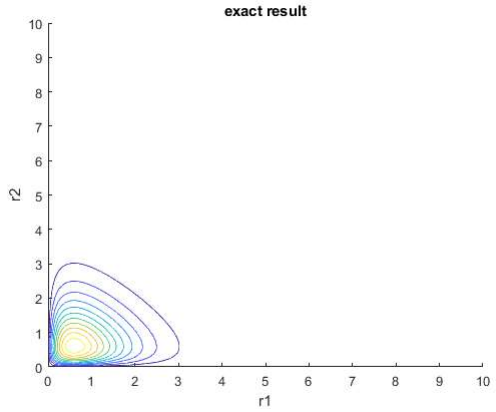

Figure 4. 29: Exact for 128 x 192.

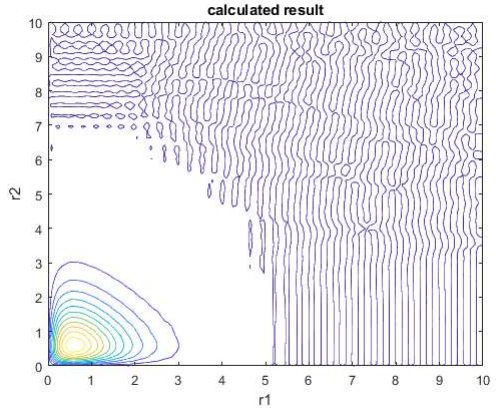

Figure 4. 30: Calculated order 1.

These does show it is possible to use the Schrödinger equation for calculations on the helium atom numerically.

Chapter 5: Conclusions and future work.

We have shown it is possible to calculate a numerical solution of the helium atom with the help of numerical methods.

This included programming in Matlab and we used the one-dimensional transport equation, the heat equation and the particle in a box solution of the Schrödinger equation for verifying the code.

The code seems fast in one-dimensional problems but quickly goes very slow for two-dimensional problems.

Trying to optimize the code or possibly use something different than Matlab is one of the possible future work.

Another is to see if it's possible to calculate on atoms in something else than the ground state and possibly extend to even more particles than the three in the helium atom.

References:

1. P. A. Tipler and R. A. Llewellyn, *Modern physics*, W.H. Freeman, New York, 2008.
2. P. W. Atkins and R. S. Friedman, *Molecular quantum mechanics*, Oxford University Press, Oxford, 2011.
3. P. C. Hemmer, *Kvantemekanikk*, Tapir akademisk forl., Trondheim, 2005.
4. A. Hinchliffe, *Molecular modelling for beginners*, Wiley, Chichester, 2008.
5. L. C. Evans, *Partial differential equations*, vol. vol. 19, American Mathematical Society, Providence, R.I, 2010.
6. B. Straughan, *The energy method, stability, and nonlinear convection*, vol. 91, Springer, New York, 2004.
7. P. D. Lax and R. D. Richtmyer, *Survey of the stability of linear finite difference equations*, Communications on Pure and Applied Mathematics **9** (1956), no. 2, 267-293.
8. H.-O. Kreiss and J. Oliger, *Comparison of accurate methods for the integration of hyperbolic equations*, Tellus **24** (1972), no. 3, 199-215.
9. H. O. Kreiss and L. Wu, *On the stability definition of difference approximations for the initial boundary value problem*, Applied Numerical Mathematics **12** (1993), no. 1, 213-227.
10. B. Gustafsson, H. Kreiss and J. Oliger, "Time dependent problems and difference methods," *Pure and Applied Mathematics*, Wiley, Hoboken, N.J., 2013.
11. D. C. Del Rey Fernández, J. E. Hicken and D. W. Zingg, *Review of summation-by-parts operators with simultaneous approximation terms for the numerical solution of partial differential equations*, Computers and Fluids **95** (2014), no. C, 171-196.
12. T. Lundquist and J. Nordström, *The sbp-sat technique for initial value problems*, Journal of Computational Physics **270** (2014), 86-104.
13. M. Svärd, *A note on $$l^{\infty }$$ l ∞ bounds and convergence rates of summation-by-parts schemes*, BIT Numerical Mathematics **54** (2014), no. 3, 823-830.
14. K. Mattsson, *Summation by parts operators for finite difference approximations of second-derivatives with variable coefficients*, Journal of Scientific Computing **51** (2012), no. 3, 650-682.
15. K. Mattsson, M. Svärd and M. Shoeybi, *Stable and accurate schemes for the compressible navier–stokes equations*, Journal of Computational Physics **227** (2008), no. 4, 2293-2316.
16. J. Gong and J. Nordström, *Interface procedures for finite difference approximations of the advection–diffusion equation*, Journal of Computational and Applied Mathematics **236** (2011), no. 5, 602-620.
17. B. Gustafsson, "High order difference methods for time dependent pde," vol. 38, Springer Berlin Heidelberg, 2008.
18. J. Nordström and T. Lundquist, *Summation-by-parts in time*, Journal of Computational Physics **251** (2013), 487-499.
19. K. Salari, P. Knupp and E. United States. Department Of, "Code verification by the method of manufactured solutions," Sandia National Laboratories, 2000.
20. C. G. Barraclough and J. R. Mooney, *Higher-order finite difference solutions of the schrödinger equation for the helium atom*, The Journal of Chemical Physics **54** (1971), no. 1, 35-44.